Fermilab

TM-954
2562.000

WIRE CHAMBERS*†

M. ATAC

Fermi National Accelerator Laboratory
Batavia, Illinois

April 1, 1980

ABSTRACT

Proportional wire chambers and drift chambers are discussed in their applications to high energy particle physics. Some results from a resistive cathode chamber and new ideas are presented.

INTRODUCTION

There have been such a variety of wire chambers built in the recent years, that it has become difficult to select the type which may be more suitable for an experiment in design. The aim of this paper is to discuss some important aspects of proportional wire chambers and drift chambers with the hope that it could be useful in decision making. Wire spark chambers are excluded in this discussion since they are well understood, and their usage has become limited. The multistep avalanche chambers will also be excluded here because they have not been used in experiments.

*Submitted to 1980 Vienna Wire Chamber Conference

†Operated by Universities Research Association under Contract with the United Stated Department of Energy.

Proportional chamber and drift chamber technology has developed rapidly since it was introduced[1,2,3] to high energy particle physics instrumentation with the parallel development of integrated circuit technology, but we are having difficulties in catching up with the development of new accelerators which have produced higher and higher energy particles at increasing rates.

The collisions of these very high energy charged particles produce large multiplicities. Fermilab is constructing a $\bar{p}p$ colliding beam facility that will produce center of mass energy of 2 TeV. Expected average charge multiplicity at this energy is about 40. Particle identification and track pattern recognition of 40 charged tracks is a very challenging problem.

Proportional Chambers

Proportional wire chambers (PWC's) are becoming less popular due to their limited spatial resolution and the high cost of large numbers of wires for large detector systems. They may still be best for handling high rates[4,5,6] in a small area. Because of the one dimensional readout nature of PWC's, a minimum of 3 wire planes must be used in determining the coordinates of more than one simultaneous track to resolve x-y ambiguities. Fig. 1 shows a typical experimental arrangement of (u, y, v) PWC planes. x-y ambiguities may not be completely resolved even with the addition of the third plane when track multiplicities are large. Fig. 2 shows the number of ambiguities as a function of the number of simultaneous tracks.[7]

An important development in the usage of PWC's has been the detection of induced pulses by cathode strips or wires which provide a precise determination[8] of the avalanche position along the anode wire (Fig. 3). Centroid determination of the induced pulses provides better than 100 μ resolution for normal tracks. An optimum geometry for strip cathodes can be

calculated[9] for achieving better resolutions. The electronic noise is the main resolution limiting factor for this type of chamber. Although it provides a bi-dimensional coordinate (x, y) readout, the coordinates are not correlated to each other for each track, thus it requires a third coordinate (u) measurement to resolve x-y ambiguity for multiple tracks. Figures 4a and 4b show 2 typical arrangements made for CELLO[10] and TASSO[11]. A σ_z = 400 μm was obtained by CELLO and a considerably less accurate σ_z resulted from the TASSO proportional chambers. 90^o strips do provide better resolution for the same strip width. As the angle is decreased from the 90^o, the resolution gets worse. Electronic noise may be the main factor for limiting the resolution when the strips are long and imperfectly shielded.

At Fermilab we have investigated[12] a similar bi-dimensional PWC using resistive cathodes of In-Sn oxide film. The induced charges were detected by printed circuit copper strips outside of the chamber volume as shown in Fig. 5. There is a 125 μm thick mylar sheet in between the resistive film and the copper strips. Local change in the charge distribution on the resistive film is detected by the copper strips as the positive ions move away from the avalanche position. Another way of saying this is that the local voltage drop in the resistive film is coupled to the copper strips capacitively. The centroid of the induced charge distribution obtained from the strips provides an excellent determination of the avalanche position along the wire. A. Michelini, CERN, used[13] this technique for obtaining a trigger common to all wires in a plane. Recently, a group[14] obtained a second coordinate from strips outside of resistive cathode tubes.

The resistive film that is used by the Fermilab group is made by Sierracin Company, California. A gas mixture of 50% A-50% C_2H_6 was bubbled through ethyl alcohol at 0° C for obtaining the following results.

Fig. 6 shows a histogram distribution of the centroids using collimated x-rays from a Fe^{55} source. The width of the collimator was 825 μm. The full width (FWHM) of the distribution agrees well with the width of the source. The distribution has a flat top within the statistics. The edges of it would give us an upper limit of 120 μm for the spatial resolution of avalanche position along the anode wires. Fig. 7 shows the centroid positions as a function of the precisely measured source positions. The linearity is excellent, and the average deviation from the straight line is less than 100 μm.

The main objective in the development of the resistive cathode PWC is to construct a resistive cathode pad chamber which can handle large numbers of simultaneous tracks at high rates in a relatively small area. A schematic picture of the high rate pad chamber is shown in Fig. 8. Small anode wire spacing, 1 mm, assures good time resolution. Our earlier results[15] obtained from 1 mm anode spacing show (Fig. 9) that a time jitter of 11 ns at full width at half maximum is achieved. A 30 ns gate width assures good efficiency.

The rate capability of an anode wire is about 10^5 cm^{-1} sec^{-1} along its length[16] using a sensitive amplifier-discriminator circuit. The space charge limits the chamber gain. Charge pile up problems may limit amplifier-discriminator front end circuitry in its rate capability when the rate exceeds 5×10^5 cm^{-1} sec^{-1} although a 10 cm long wire can handle rates of 10^6 sec^{-1}. This would not be a problem when 10 independent pads observe the

avalanches along the wire as in this scheme. The distribution of charges collected from the pads indicate the hit wire and the avalanche position along the wire. The electronic noise for each pad channel should be small due to the small capacitance of each pad.

The charge obtained from each pad can be digitized by a flash ADC[17] (FADC) and stored into a memory every 32 ns until an interesting event is found. Then the centroid of the charge distribution along the wire (mainly 3 pads contribute) measures the avalanche position along the anode wire. As we have seen from the strip chamber results, this coordinate can be measured to an accuracy of better than 120 μm. The centroid of the charge distribution orthogonal to the wire determines the hit wire. A careful look at this distribution could give us which side of the wire the avalanche occurred. The accuracy of this coordinate is then measured to about σ_{rms} = 300 μm ($1/\sqrt{12}$ for wire spacing of 1 mm). This x-y coordinate measurement is completely unambiguous and provides space points for all resolvable simultaneous tracks. FADC's speed of 32 ns, matching the gate width of 30 ns, gives us a rate capacility of > 3 x 10^7 counts per second for an area of 10 cm x 10 cm for a large number of simultaneous tracks.

Drift Chambers

Drift chambers have become the most widely used wire chambers since they were introduced to high energy physics instrumentation[2,3] by the G. Charpak-F. Sauli and J. Heintze-A. H. Walenta groups. Drift chambers have taken a variety of shapes and dimensions since. Historic development is well summarized by J. Heintze[18]. Only certain aspects of drift chambers will be discussed in the following.

Drift chambers provide high spatial resolution[16], 100-200 μm at atmospheric pressures. A careful study of drift velocity as a function of the electric field can improve the resolution to 50-80 μm[19] for a drift spacing of 2 cm. Spatial resolution of 20 μm are obtainable at high pressures[20].

During the last few years, exciting high energy physics experiments have been carried out using colliding beams at SPEAR, DORIS, ISR, PETRA, and Cornell. More experiments are planned at PEP, CERN $\bar{p}p$ at 540 GeV center of mass energy, Fermilab $\bar{p}p$ at 2 TeV, and ISABELLE. The detectors for these experiments, largely drift chambers, cover almost 4π steradians and detect rather large numbers of simultaneous tracks (up to 40 charge tracks on the average). Space point determination of tracks help improve pattern recognition and save a great deal of computing time. A. Wagner from the JADE[21] experiment reported that correlated bi-dimensional coordinate determination untangled complicated events.

Mainly there are 2 techniques for obtaining correlated bi-dimensional coordinate readout with drift chambers, charge division[22,23] and delay-line readout[24].

Some charge division and delay line results published by various experimental groups are listed in Tables 1 and 2. They indicate that the delay lines provide about a factor of 4 better resolution on the average than charge division. It is not clearly understood what limits the resolution in charge division. Electronic noise, cross-talk between the sense wire, and the cathode wires, and reflections due to imperfect termination could be some of the resolution limiting factors in the charge division readout technique. It appears that signal to noise is the major factor in limiting the resolution for the delay line technique.

The noise limit factor calculated using V. Radeka's formula[25] for Fermilab's printed circuit delay line drift chamber is in good agreement with the obtained results.

$$\frac{\Delta L}{L} \sim 2.46 \left(\frac{\tau_F}{\tau_D}\right) \left(\frac{e_n}{Z_o Q_D}\right) \tau_F^{1/2}$$

The parameters for the Fermilab delay-line drift chambers are:

$$\tau_F = 30 \text{ ns}, \ \tau_D = 277 \text{ ns/1.5 m}, \ Z_o = 85\Omega, \text{ and } Q_D = 3 \times 10^5 \ e^-.$$

σ_{rms} = 0.2% of the length of the line, giving σ_{rms} = 3 mm.

Multitrack Resolution

How do these most commonly used correlated bi-dimensional drift chambers, one using charge division and the other using delay line readout, compare in two-track resolution? One way to answer this question is to compare confusion (or dead) region around the anode wires during the detection of a track by the two techniques.

Using the charge division technique, the charges from each end of the anode wire are integrated for about 150-200 ns for obtaining a σ_{rms} resolution of 1% over the wire length. This results in a 2 L cm^2 (where L is the wire length) of confusion area for an electron drift rate of 200 ns/cm in the gas. This is schematically shown in Fig. 10.

For the delay line technique, let us take Fermilab drift chambers using the printed circuit delay line. This delay line produces pulses of 6 ns rise time with a full width of less than 50 ns into 85 Ω impedance (characteristic impedance of the delay line) using 50% argon - 50% ethane gas, bubbled through

ethyl alcohol at 0^{o} C (about 5% admixture of ethyl alcohol). It is a balanced line, and the measured noise into 85 Ω is less than 30 μV through a balanced to unbalanced transformer which cancels common mode noise.

In this case, the results are indicated in Fig. 11. The maximum confusion area is 1.5 cm^2 which is less than 1% of the area of the charge division case. The double pulses obtained from each end of the delay line are resolved in time if they come about a minimum of 50 ns apart. This implies a minimum track separation of 2.5 mm with the electron drift time of 200 ns/cm in the gas.

Footnotes

1. G. Charpak, R. Bouclier, T. Bressani, J. Favier, and C. Zupancic, Nucl. Instr. and Meth. 62 (1968) 262.

2. G. Charpak, D. Rahm, and H. Steiner, Nucl. Instr. and Meth. 80 (1970) 13.

3. A. H. Walenta, J. Heintze, B. Schurlein, Nucl. Instr. and Meth. 92 (1970) 373.

4. W. Frieze et. al., Nucl. Instr. and Meth. 136 (1976) 93.

5. R. Hammarstron, O. Runolfsson, and M. Uldry, 1980 Vienna Wire Chamber Conference Report.

6. R. J. Gray, 1980 Vienna Wire Chamber Conference Report.

7. R. Raja, Fermi National Accelerator Laboratory, private communication.

8. G. Charpak and F. Sauli, Nucl. Instr. and Meth. 113 (1975) 381.

9. E. Gatti, A. Longoni, H. Okuno, and P. Semenza, Nucl. Instr. and Meth. 163 (1979) 83-92.

10. Private communication with the CELLO Group.

11. Private communication with the TASSO Group.

12. M. Atac, Fermilab Internal Report TM-932 (January 1980) and M. Atac, D. Hanssen, and J. Urish, will be published.

13. A. Michelini, CERN, private communication.

14. G. Battistoni, E. Iarocci, G. Nicoletti, L. Trasatti, reported at the 1980 Vienna Wire Chamber Conference.

15. M. Atac, IEEE Trans. Nucl. Sci. No. 3, Vol. NS-19 (1972) 144.

16. A. Breskin, G. Charpak, F. Sauli, M. Atkinson, and G. Schultz, Nucl. Instr. and Meth. 124 (1975) 189.

17. B. Hallgren and H. Verweij, IEEE Trans. Nucl. Sci.

18. J. Heintze, Nucl. Instr. and Meth. 156 (1978) 227-244.

19. N. A. Filatova, T. S. Nigmanov, V. P. Pugachevich, V. D. Riabtsov, M. D. Shafranov, E. D. Tsyganov, D. V. Uralsky, A. S. Vodopianov, F. Sauli, and M. Atac, Nucl. Instr. and Meth. 143 (1977) 17-28.

20. W. Farr, J. Heintze, K. H. Hellenbrand, and A. H. Walenta, Nucl. Instr. and Meth. 154 (1978) 175-181.

21. H. Drumm, R. Eichler, B. Granz, J. Heintze, G. Heinzelmann, R. D. Heuer, J. Von Krogh, P. Lennert, T. Nozaki, H. Rieseberg, A. Wagner, and P. Warming, Proceedings of 1980 Vienna Wire Chamber Conference.

22. H. Foeth, R. Hammerstrom, and C. Rubbia, Nucl. Instr. and Meth. 109 (1973) 521.

23. V. Radeka, IEEE Trans. Nucl. Sci. 21 (1974) 51.

24. A. Breskin, G. Charpak, F. Sauli, and J. Santiard, Nucl. Instr. and Meth. 119 (1974) 1.

25. V. Radeka and P. Rehak, IEEE Trans. Nucl. Sci. 25 (1978) 46.

26. V. Radeka, IEEE Trans. Nucl. Sci., Vol. NS-21, No. 1 (1974).

27. A. Dwurazny, L. Hajduk, Z. Hajduk, H. Palka, M. Turala, E. Lorenz, R. Richter, and J. Turnau, Nucl. Instr. and Meth. 156 (1978) 245.

28. M. Claveti et. al., Proceedings of 1980 Vienna Wire Chamber Conference.

29. A. Breskin, G. Charpak, F. Sauli, and J. C. Santiard, Nucl. Instr. and Meth. 119 (1974) 1.

30. M. Atac and J. Urish, Nucl. Instr. and Meth. 156 (1978) 163.

31. L. Camilleri et. al., Nucl. Instr. and Meth. 156 (1978) 275.

32. D. Achterbert et. al., Nucl. Instr. and Meth. 156 (1978) 287.

33. A. Bechini et. al., Nucl. Instr. and Meth. 156 (1978).

Table I

Current Division Characteristics

Number and Reference	Wire Length (cm)	Resistance ohm/m	σ_{rms} (cm)
22 H. Foeth et. al.	10	720	0.2
26 V. Radeka et. al.	240	2350	0.5-1.2
18 J. Heintze et. al.	250	300	1.6
27 A. Dwurazny et. al.	60	2000	0.6
28 M. Clavetti et. al.	250		1.5-2 using FADC

Table 2

Delay Line Characteristics

Number and Reference		Type	Impedence ohm	DC Resistance ohm/m	Delay ns/cm	Length cm	σ_{rms} mm
29	G. Charpak et. al.	Wound	1300	160	1.3	150	2-3.5
30	M. Atac et. al.	Printed	85	40	1.85	150	3-4
31	L. Camilleri et. al.	Wound	550	110	2.3	150	5
32	O. Achterberg et. al.	Wound	325	22	3.66	100	4
33	A. Bechini et. al.	Wound	1200	580	7.43	50	2

Figure Captions

Fig. 1 — A typical stereo arrangement of three proportional wire chamber planes.

Fig. 2 — Number of multitrack ambiguities as a function of simultaneous track multiplicities.

Fig. 3 — Bi-dimensional proportional wire chamber with readout cathode strips.

Fig. 4a and b — Cathode strip readout arrangements for CELLO and TASSO cylindrical proportional chambers, respectively.

Fig. 5 — Resistive cathode readout bi-dimensional proportional wire chambers.

Fig. 6 — Histogram distribution of centroid measurements using a collimated Fe^{55} x-ray source.

Fig. 7 — Centroid positions versus source positions.

Fig. 8 — Resistive cathode chamber with pad readout for high rate readout capability.

Fig. 9 — Time distribution of tracks from a 1 mm anode wire spacing of a proportional wire chamber.

Fig. 10 — Schematic description of charge division readout technique.

Fig. 11 — Multitrack resolution from Fermilab delay line readout.

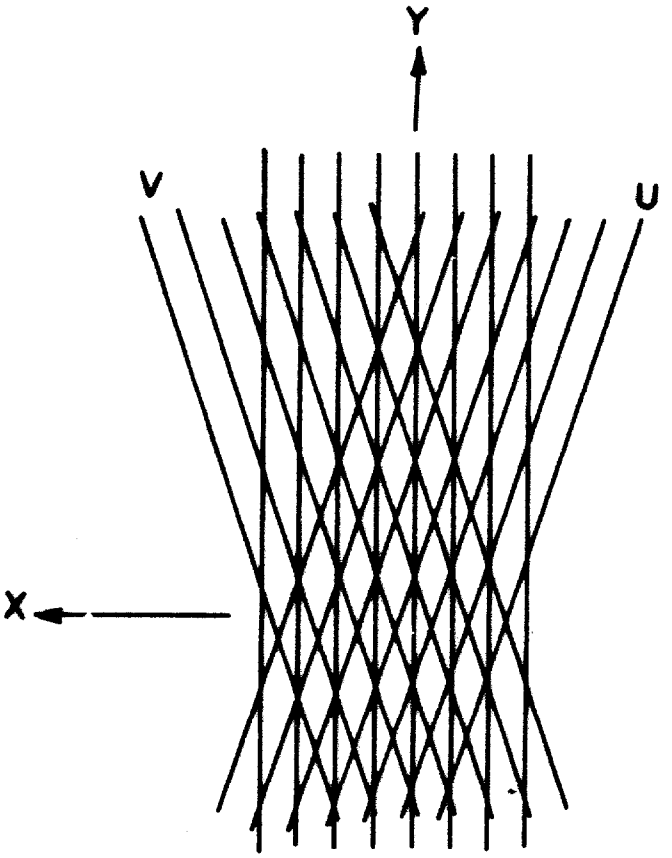

FIG. 1

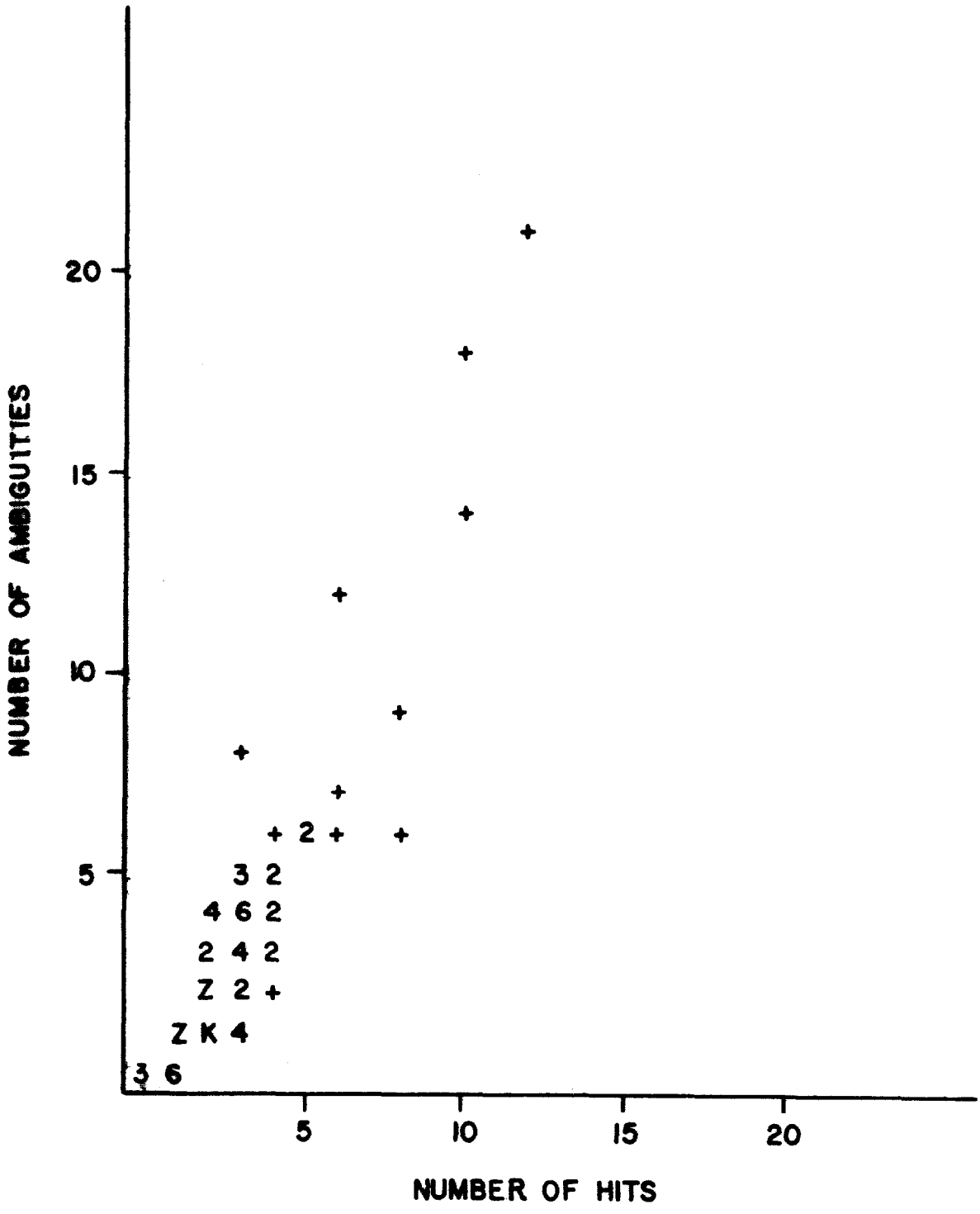

FIG. 2

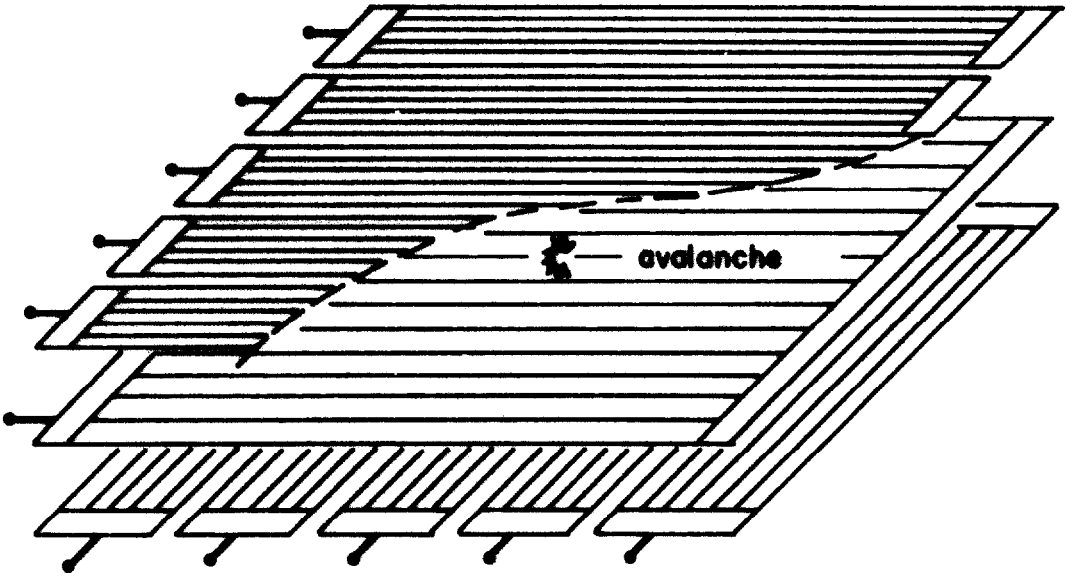

FIG. 3

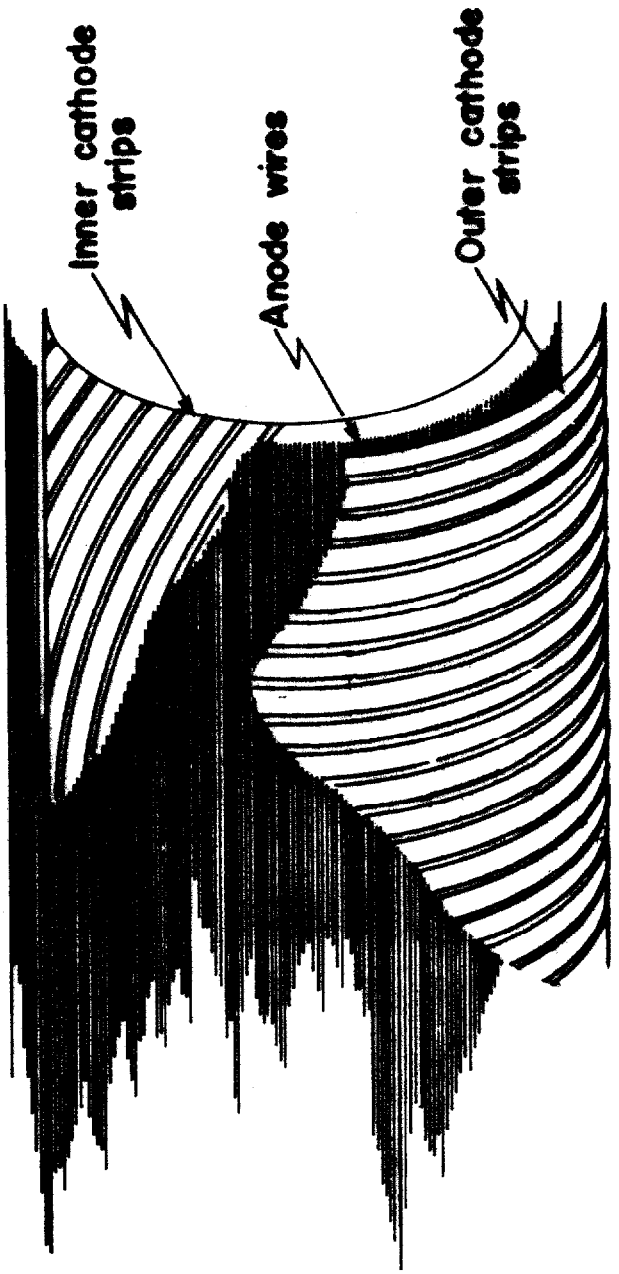

FIG. 4a

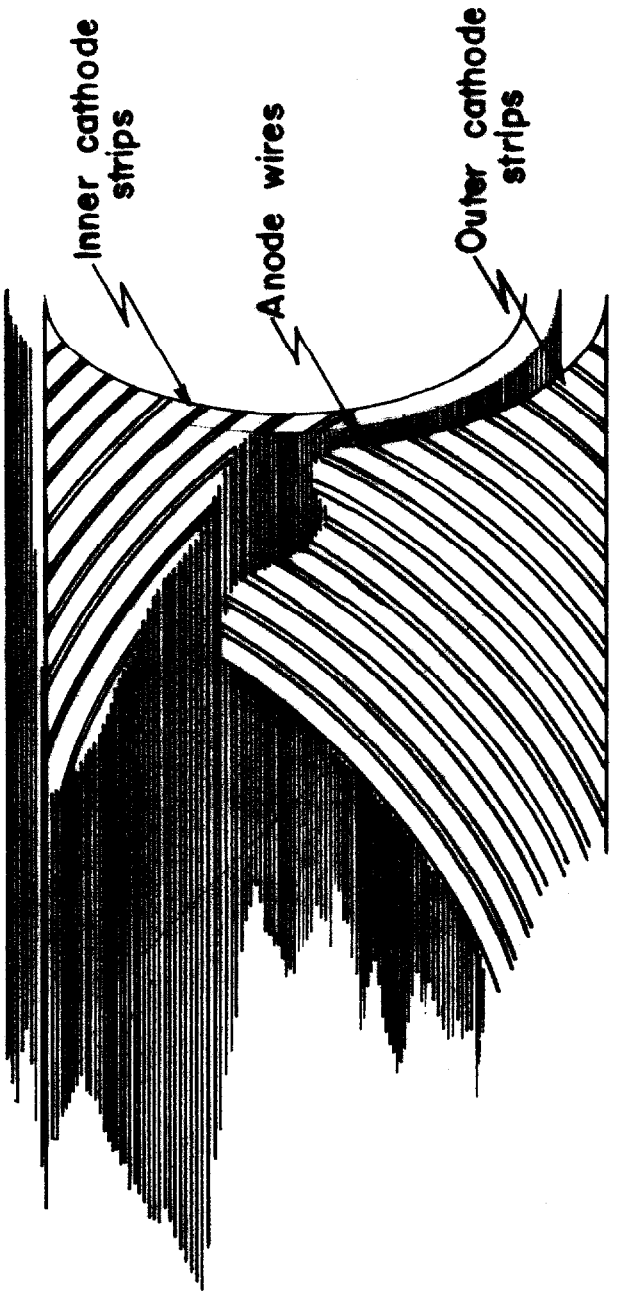

FIG. 4b

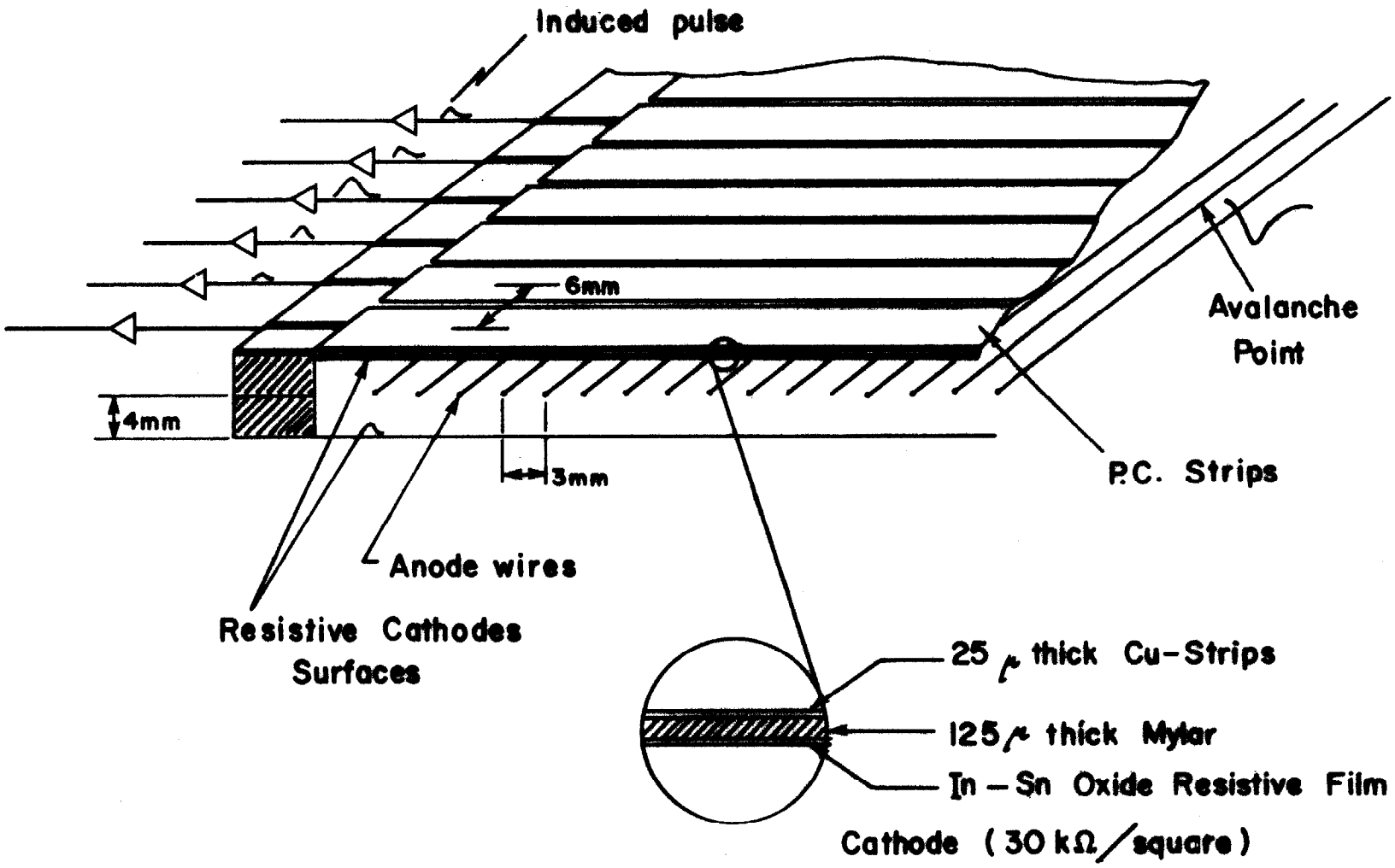
Induced pulse
6mm
Avalanche
Point
4mm
3mm
P.C. Strips
Anode wires
Resistive Cathodes
Surfaces
25 μ thick Cu-Strips
125 μ thick Mylar
In – Sn Oxide Resistive Film
Cathode (30 kΩ/square)

FIG. 5

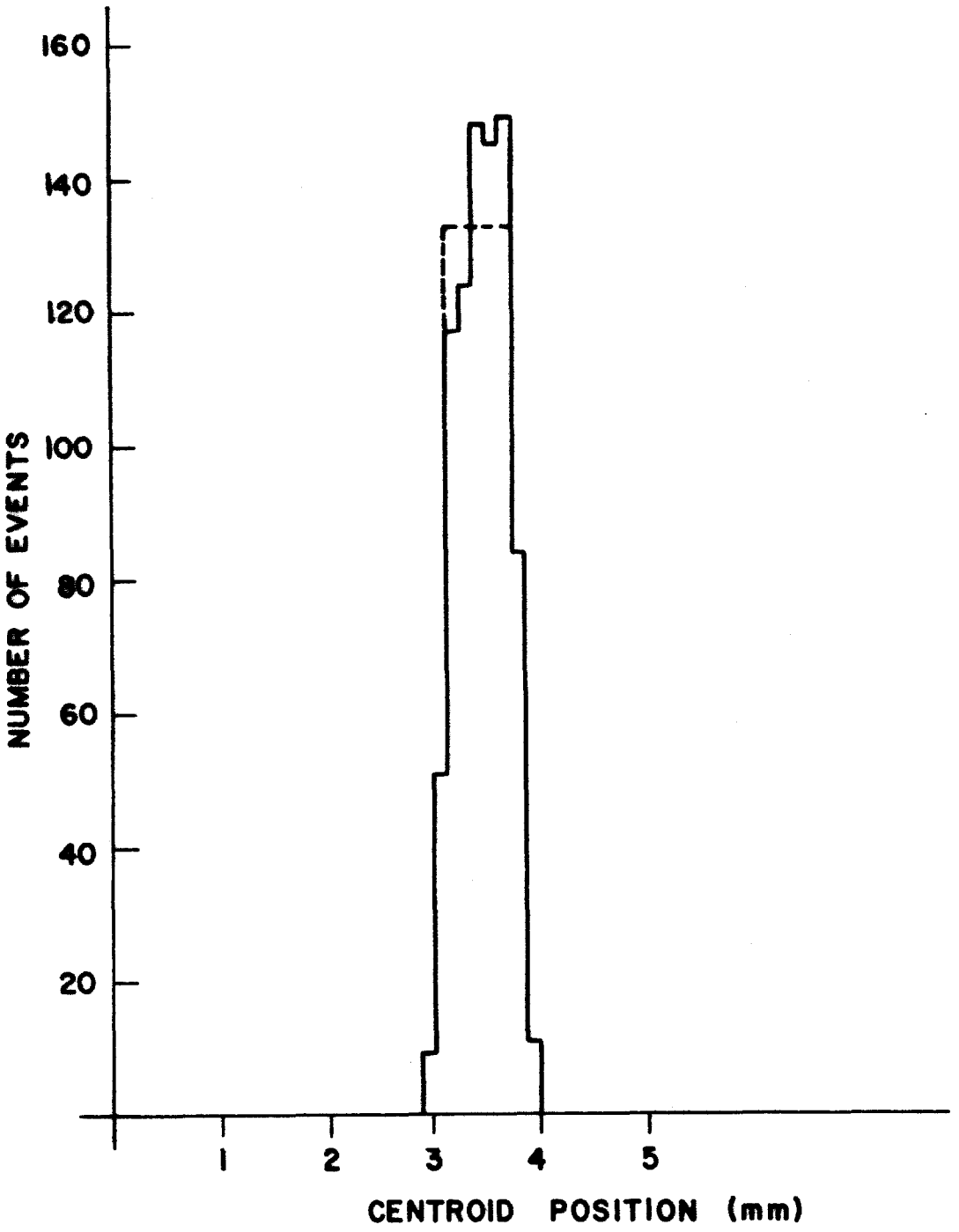
160
140
120
100
80
60
40
20
NUMBER OF EVENTS
1
2
3
4
5
CENTROID POSITION (mm)

FIG. 6

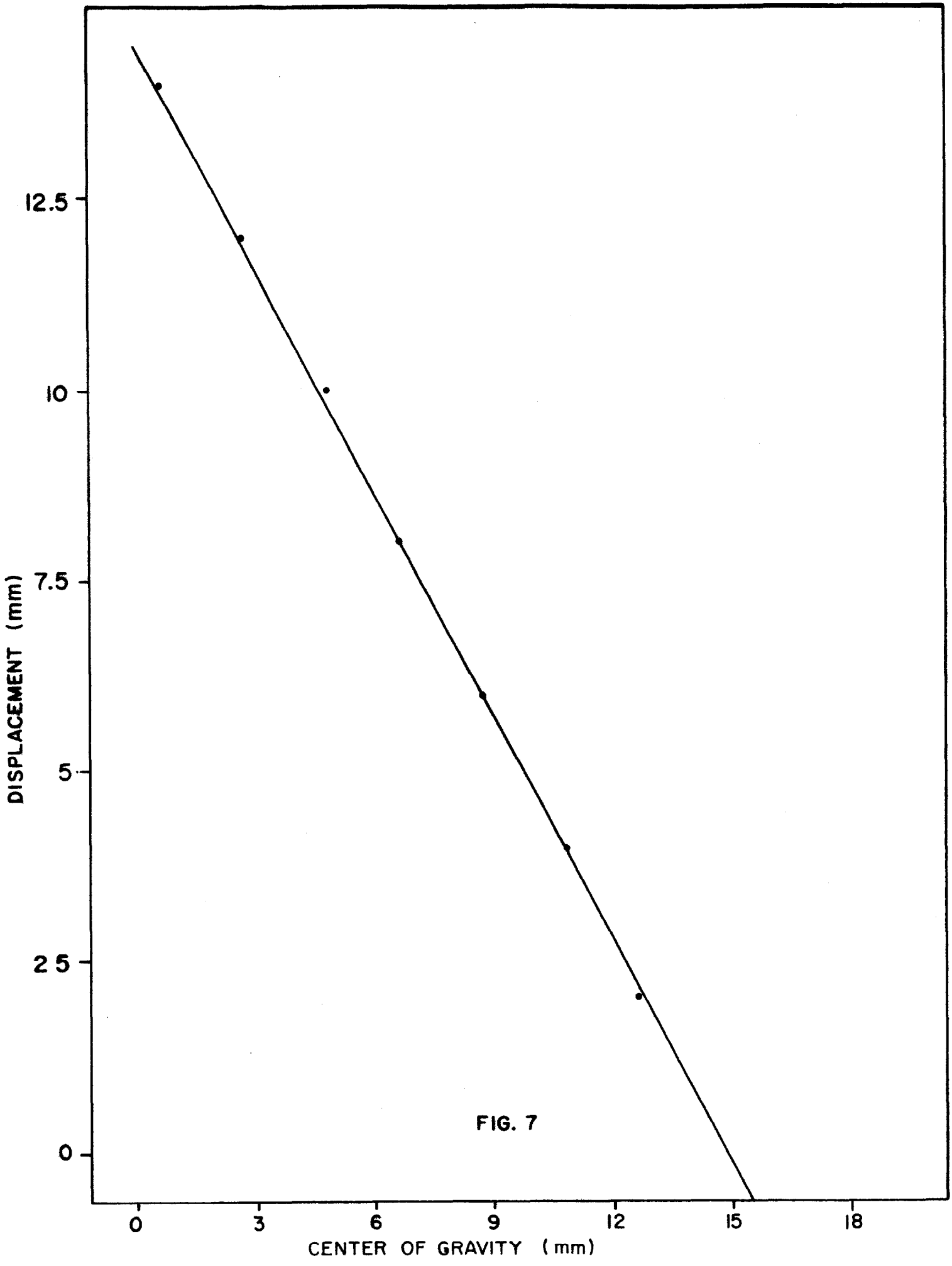
12.5
10
7.5
5
2.5
0
DISPLACEMENT (mm)
0
3
6
9
12
15
18
CENTER OF GRAVITY (mm)

FIG. 7

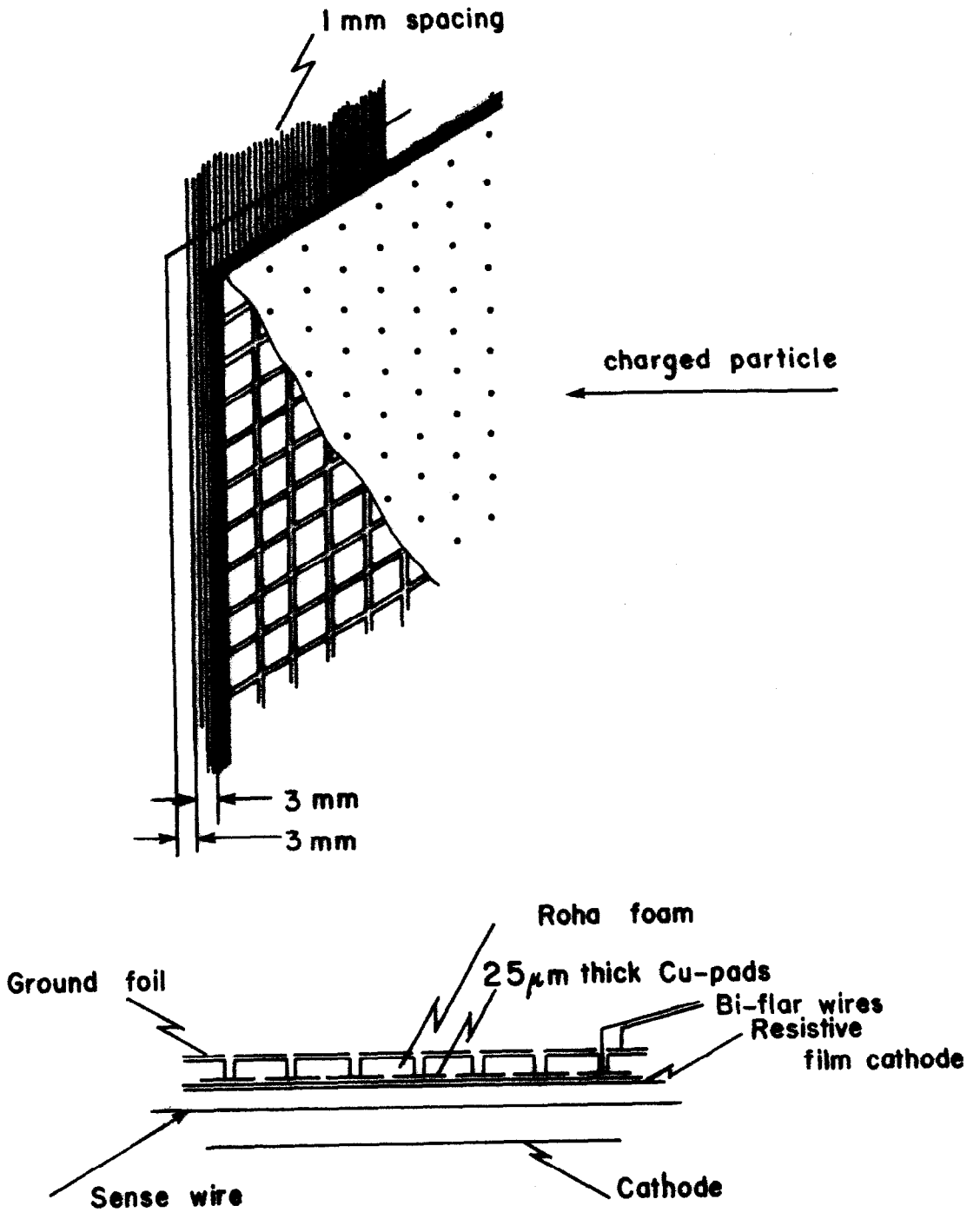
1 mm spacing
charged particle
3 mm
3 mm
Roha foam
25μm thick Cu-pads
Ground foil
Bi-flar wires
Resistive
film cathode
Sense wire
Cathode

FIG. 8

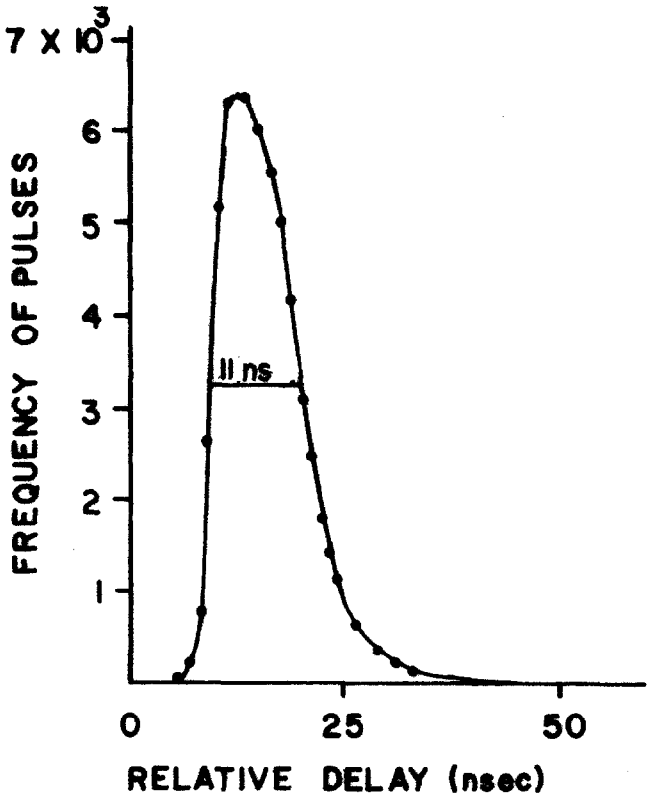
7 X 10³
6
5
4
3
2
1
FREQUENCY OF PULSES
11 ns
0
25
50
RELATIVE DELAY (nsec)

FIG. 9

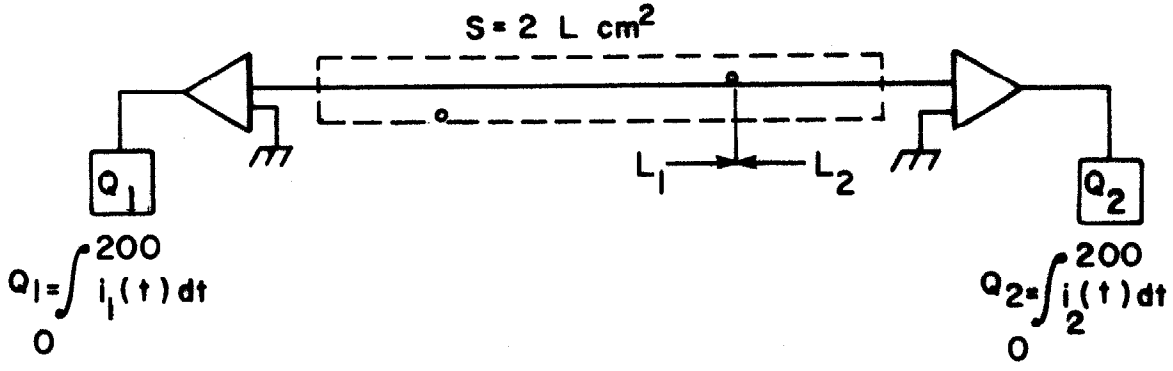

FIG. 10

FERMILAB DELAY-LINE DRIFT CHAMBER

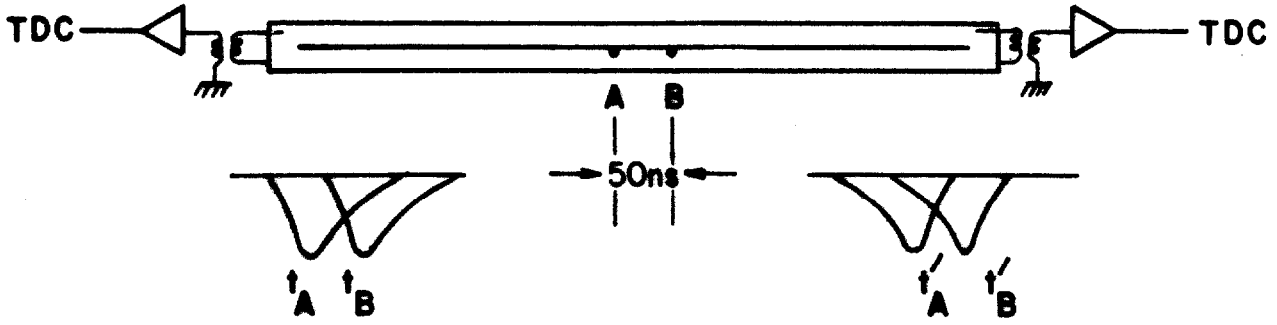

$$t_A + t'_A = t_B + t'_B = \text{const.}$$

$$\tau_{delay} = 1.85\ ns/cm$$

$$\tau_{drift} = 200\ ns/cm$$

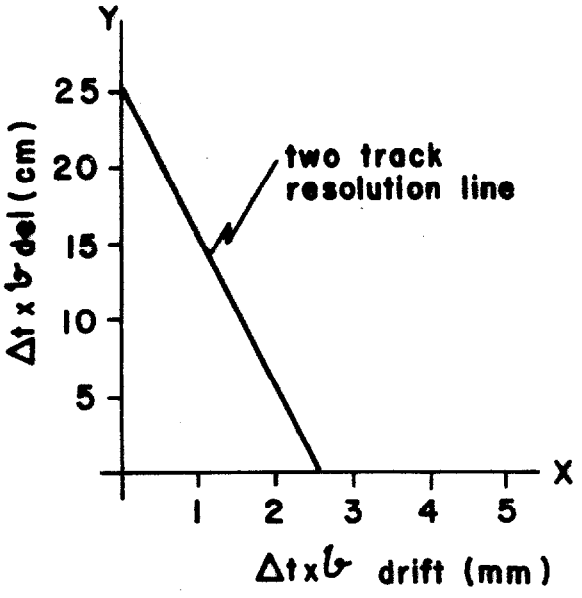

ΔX (mm)	ΔY (cm)	Dead area (cm^2)
1	15	1.5
2	5	1
2.5	0	0

FIG. 11